H), 1.55-1.20 (m, 15 H), 0.90 (t, $J$ = 7.0 Hz, 3 H). Anal. Calcd for $C_{13}H_{23}NO_4$: C, 60.68; H, 9.01; N, 5.44. Found: C, 60.85; H, 8.97; N, 5.44.

***N*-[(*tert*-Butyloxy)carbonyl]-*trans*-3-*n*-propyl-D-proline (14b).** Amide **13b** (>99% diastereomeric purity) was converted similarly to **14b**: mp 90-92 °C (hexane); $[\alpha]^{24}_D$ = +43.2° (*c* 1.0, $CHCl_3$).

**Acknowledgment.** We thank Dr. Stephen Spanton for performing the X-ray analysis, David Whittern for carrying out many NMR experiments, Prof. Henry Rapoport for useful discussions regarding the stereochemical assignments, and Dr. Fatima Basha for the preparation of authentic *N*-benzyl-3(*S*)-phenylpyrrolidine.

**Registry No.** **1a**, 123724-21-0; **1b**, 123724-22-1; **2a**, 3005-63-8; **2b**, 123724-23-2; **4**, 123724-24-3; *cis*-**5**, 123807-01-2; *trans*-**5**, 123807-02-3; **7**, 123807-03-4; **8**, 123724-25-4; *cis*-**9**, 123724-26-5; *trans*-**9**, 123724-27-6; **11**, 123877-36-1; **12a**, 123724-28-7; **12b**, 123724-29-8; **13a**, 123724-30-1; **13b**, 123724-31-2; **14a**, 123724-32-3; **14b**, 123724-33-4; (-)-MTPA-Cl, 39637-99-5; (*S*)-(-)-PhCH(Me)$NH_2$, 2627-86-3; (*S*)-(+)-HOOCCH(Ph)$CH_2$COOH, 4036-30-0; $AcNHCH(COOEt)_2$, 1068-90-2; (*E*)-$H_3CCHCHCH_2CH_2CH_3$, 6728-26-3; (*S*)-(-)-PhCH(Me)$NH_2$·HCl, 17279-30-0; D-*trans*-3-phenylproline, 118758-50-2; (*S*)-(+)-3-phenylpyrrolidine, 62624-46-8; (*S*)-(*R**,*R**)-*N*-[[α-methoxy-α-(trifluoromethyl)phenyl]-acetyl]-3-phenylpyrrolidine, 123724-34-5; (*S*)-*N*-benzyl-3-phenylpyrrolidine, 59349-74-5; (*R*)-3-phenylpyrrolidine, 61586-46-7; (±)-*cis*-3-*n*-propylproline hydrochloride, 123807-04-5; (±)-*trans*-3-*n*-propylproline hydrochloride, 123807-05-6; (±)-*cis*-3-*n*-propylproline methyl ester hydrochloride, 123724-35-6; (±)-*trans*-3-*n*-propylproline methyl ester hydrochloride, 123724-36-7.

**Supplementary Material Available:** List of positional and anisotropic thermal parameters of non-hydrogen atoms, positional and thermal parameters of hydrogen atoms, and bond distances and bond angles for compound **12b** (5 pages). Ordering information can be found on any current masthead page.

# Urocanic Acid Photobiology. Identification and Characterization of the Major Photoadducts Formed between Urocanic Acid and Thymidine[1]

Sherry J. Farrow,[†] Claude R. Jones,[†] Daniel L. Severance,[†] Rose M. Deibel,[†] William M. Baird,[‡] and Harry A. Morrison*,[†]

*Department of Chemistry and Department of Medicinal Chemistry, Purdue University, West Lafayette, Indiana 47907*

*Received August 2, 1989*

Two products (adducts I and II), formed under conditions known to photochemically bind urocanic acid (UA) covalently to DNA, have been isolated from the photolysis of UA and thymidine. The gross structural features of the adducts were determined by using photolytic cleavage, mass spectrometry, UV absorption spectroscopy, $^1H$ and $^{13}C$ NMR, and $^1H$-$^{13}C$ correlation spectroscopy (COLOC). The regiochemistries were assigned on the basis of the pH dependence of hydrogen chemical shifts. The relative stereochemistries were determined by using nuclear Overhauser effects and spin-lattice relaxation times. All of these data support the assignment of the adducts as diastereomerically related cyclobutane structures resulting from 2 + 2 cycloaddition of the UA acrylic acid and thymidine double bonds.

Urocanic acid (2-propenoic acid, 3-(1*H*-imidazol-4-yl)-, UA, Figure 1) is a major component of the stratum corneum and recently has been a subject of intense photobiological interest.[2] Early studies hypothesized the biological role of UA as both a natural sunscreen and a photoprotecting agent against UV damage to DNA.[2] It is a major absorber of UV light in the skin and has been found to undergo efficient $E/Z$ isomerization as its primary, unimolecular photochemical reaction.[2] UA is also quite reactive with singlet oxygen[2] and has been shown to photolytically generate superoxide.[3] However, more recent work has emphasized the potential deleterious effects of UA when exposed to UV light and has focused on the direct photochemical interaction of UA and biologically important components. Examples are the UA-sensitized photoinactivation of bacteriophage G4 single-stranded DNA[4] and the photochemical incorporation of UA into bovine serum albumin.[5] It has been determined that UA photochemically binds to native calf thymus DNA when these are irradiated at λ > 270 nm, with some evidence that one of the bases responsible for the photochemical incorporation is thymidine.[6] In addition, two independent studies have found that irradiated samples of (*E*)-UA can cause immune suppression in mice (there is good evidence that the causative agent is (*Z*)-UA)[7] and may increase the animals' susceptibility to cancer.[8] The results of these studies suggest that UA photochemistry may be important to the phenomenon of photocarcinogenesis. The present

[†] Department of Chemistry.
[‡] Department of Medicinal Chemistry.

(1) Organic Photochemistry. 80. Part 79: Maxwell, B. D.; Nash, J. J.; Morrison, H. A.; Falcetta, M. L.; Jordan, K. D. *J. Am. Chem. Soc.*, in press. Abstracted, in part, from the Doctoral Dissertation of Sherry Farrow, Purdue University, December, 1988. Presented, in part, at the 15th Annual Meeting of the Americal Society for Photobiology, June 21-25, 1987, Bal Harbour, FL.

(2) For reviews see: (a) Morrison, H. A.; Deibel, R. M. *Photochem. Photobiol.* **1986**, *43*, 663-665. (b) Morrison, H. A. *Photodermatology* **1985**, *2*, 158-165.

(3) Morrison, H. A.; Deibel, R. M. *Photochem. Photobiol.* **1988**, *48*, 153-156.

(4) Tessman, I.; Morrison, H. A.; Bernasconi, C.; Pandey, G.; Ekanayake, L. *Photochem. Photobiol.* **1983**, *38*, 29-35.

(5) Deibel, R. M.; Morrison, H. A.; Baird, W. M. *Photochem. Photobiol.* **1987**, *45*, 421-423.

(6) Morrison, H. A.; Mauclair, B.; Deibel, R. M.; Pandey, G.; Baird, W. M. *Photochem. Photobiol.* **1985**, *41*, 251-257.

(7) De Fabo, E. C.; Noonan, F. P. *J. Exp. Med.* **1983**, *157*, 84-98. Noonan, F. P.; De Fabo, E. C.; Morrison, H. A. *J. Invest. Dermatol.* **1988**, *90*, 92-99, and references therein. Ross, J. A.; Howie, S. E. M.; Norval, N.; Maingay, J.; Simpson, T. J. *J. Invest. Dermatol.* **1986**, *87*, 630-633.

(8) Reeve, V. E.; Greenoak, G. E.; Canfield, P. J.; Boehm-Wilcox, C.; Gallagher, C. H. *Photochem. Photobiol.* **1989**, *49*, 459-464.

0022-3263/90/1955-0275$02.50/0 

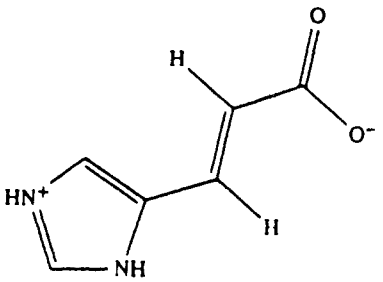

**Figure 1.** (*E*)-Urocanic acid.

investigation has, therefore, focused on the photochemical reaction of UA and thymidine in an effort to identify the possibile DNA lesions generated by UA. Included in this report are the identification, isolation, and characterization of two major photoproducts formed between UA and thymidine under conditions known to photochemically incorporate UA into DNA. To date, these are the only photoproducts formed between UA and DNA nucleosides that have been isolated and characterized.

## Experimental Section

**Materials.** (*E*)-UA, thymidine, *Pseudomonas fluorescens* cells (from which histidase was extracted), alumina type 305, Dowex 50×-8-400, and 3-(trimethylsilyl)-1-propanesulfonic acid (DSS) were from Sigma. L-Histidine, cyclobutanecarboxylic acid, 20 wt % DCl in $D_2O$, and 99.8% D $D_2O$ were from Aldrich; 99.996% D deuterium oxide was from Cambridge Isotope Laboratories. 2-Mercaptoethanol was from Kodak. L-[*ring*-2-$^{14}$C]Histidine (SA = 52 mCi/mmol) was from Research Products International. ACS scintillation fluid was from Amersham. All water was deionized and distilled by using a Corning MP-1 distillation apparatus. All other chemicals were reagent grade.

**Instrumentation.** UV spectra were recorded on a Hewlett-Packard HP8451A photodiode array spectrometer. NMR spectra of samples in 99.996% D $D_2O$ were obtained by using a Nicolet NT-470, a General Electric QE-300, or a Varian XL-200 spectrometer and were referenced by using either DSS or the HDO resonance of the solvent at $\delta$ 4.76. High-resolution mass spectra were performed on compounds in a glycerol matrix by using a Kratos MS-50 mass spectrometer. Measurements of pH were done using a Corning 125 meter standardized with Sargeant Welch buffer solutions (pH 4, 7, and 10); measurements in $D_2O$ are direct meter readings, are uncorrected, and are given as pH*.

**Photolyses.** Photolyses were done using 8-mL quartz phototubes in a turntable with either a Canrad-Hanovia 450-W medium-pressure Hg lamp, Model 679A-36, encased with a Corex filter ($\lambda > 270$ nm; $6 \times 10^{16}$ $h\nu$/s) or a Canrad-Hanovia low-pressure Hg lamp ($\lambda = 254$ nm; (2–3) $\times 10^{16}$ $h\nu$/s), Model 688A-45. Laser photolyses at $\lambda = 308$ nm were done using a XeCl-charged Lambda Physik EMG 101 excimer laser, a fluid-cooled, black aluminum cuvette holder (1 cm$^2$), an uncoated optical quartz cylindrical plano-convex lens (38 mm × 102 mm focal length) from Esco Products, and a Masterline 2096 cooling bath from Forma Scientific. The laser was operated at 10 Hz and 29.9 kV. Samples were photolyzed in a 1-cm$^2$ quartz cuvette 48 cm from the laser beam port with the focusing lens 11 cm from the face of the cuvette and oriented with the cylindrical axis vertical in order to provide horizontal focusing. The light intensity was determined by using uranyl oxalate actinometry.[9]

**Reverse-Phase HPLC.** The HPLC system consisted of Varian 5000 liquid chromatograph with ternary capability, a Varian 2050 variable-wavelength detector (set at 254 nm unless specified otherwise), a Rheodyne 7125 injection valve with either a 2.0-mL or a 0.2-mL injection loop, and a Perkin-Elmer LCI-100 computing integrator. Analyses were done using an Alltech C-8 analytical column (4.6 cm × 25 cm), an Alltech C-8 semipreparative column (10 mm × 25 cm), or a Hamilton PRP-1 analytical column (4.6 mm × 25 cm) with one of the following HPLC methods: (A) 93:7 ratio of 40 mM phosphate buffer (pH = 6) to methanol with a flow rate of 0.3 mL/min for the first 15 min and 1.0 mL/min for the ensuing 15 min; (B) identical with method A except a 94:6 ratio of buffer to methanol was used; (C) 100% 20 mM phosphate buffer (pH = 6) flowing at 3.0 mL/min; (D) 99:1 ratio of 40 mM phosphate buffer (pH = 6) to methanol from 0 to 15 min, a 1–10% methanol gradient from 15 to 25 min, and a 10–1% methanol gradient from 25 to 35 min with a flow rate of 3.0 mL/min; (E) 100% 40 mM phosphate buffer (pH = 6) from 0 to 15 min, a 0–20% methanol gradient from 15 to 35 min, and a 20–0% methanol gradient from 35 to 50 min with a flow rate of 1.0 mL/min; (F) 100% 40 mM phosphate buffer (pH = 6) with a flow rate of 2.5 mL/min; (G) 100% 50 mM phosphate buffer (pH = 7) with a flow rate of 1.0 mL/min. Initial isolation of the UA–thymidine adducts was done with a Bioanalytical Systems LC-1200 Miniprep apparatus using a Lichoprep RP-8 size B (310-25) LoBar column, an Isco detector set at 254 nm, and a Hewlett-Packard 3390 integrator. The eluent was 20 mM ammonium acetate and 1% acetonitrile at a flow rate of 3 mL/min. For radioactive samples, $^{14}$C was assayed by collecting fractions with an Isco fraction collector, mixing each fraction with 4 mL of ACS scintillation fluid, and counting DPM on a Packard 300C liquid scintillation counter.

**Preparation of (*E*)-[*ring*-2-$^{14}$C]UA.** (*E*)-[*ring*-2-$^{14}$C]UA was prepared from (*L*)-[*ring*-2-$^{14}$C]histidine by using a method previously described.[6] The enzymatic deamination resulted in 90% conversion, and the isolated yield of (*E*)-[*ring*-2-$^{14}$C]UA (SA = 11.2 mCi/mmol) was 58%. Prior to use, the (*E*)-[*ring*-2-$^{14}$C]UA was purified by HPLC using an Alltech C-8 column (4.6 mm × 25 cm) and HPLC Method G. (*E*)-[*ring*-2-$^{14}$C]UA was collected at 4.1 min (4.1 mL).

## Results and Discussion

**A. Isolation of the UA–Thymidine Photoproducts and Their Initial Chemical and Spectral Characterization. (i) Photolysis of (*E*)-[*ring*-2-$^{14}$C]UA and Thymidine.** The photochemical reaction of (*E*)-UA and thymidine was initially investigated by using conditions known to produce photochemical incorporation of (*E*)-UA into DNA. A 2-mL solution of thymidine (10 mM) and (*E*)-[*ring*-2-$^{14}$C]UA (4 mM; SA = $2.7 \times 10^{-2}$ mCi/mmol) in 0.1 M phosphate buffer (pH = 7) was irradiated at 10 °C for 48 h by using a Corex-filter medium-pressure Hg lamp. Analysis by HPLC using the Hamilton PRP-1 column showed two major products in addition to unreacted thymidine and isomerized UA. One product, UA–thymidine adduct I, appeared at 10.1 min (3.0 mL) by using HPLC method B and comprised 12% of the total radioactivity (15% yield). A second product, UA–thymidine adduct II, appeared at 12.2 min (3.7 mL) by using HPLC method A and comprised 16% the total radioactivity (20% yield). With use of both HPLC analyses, the amount of unreacted (*E*)- and (*Z*)-UA was calculated to be 18%.

**(ii) Isolation of the UA–Thymidine Products.** Both major UA–thymidine products were isolated by using reverse-phase HPLC. Solutions containing (*E*)-UA (6 mM) and thymidine (10 mM) in 84 mL of 0.1 M phosphate buffer (pH = 7) were irradiated at 10 °C for 116 h by using a Corex-filtered medium-pressure Hg lamp. The photolysis solutions were lyophilized to a volume of 12 mL, resulting in the precipitation of phosphate salts. After filtration of the solutions, separation was initially achieved using LoBar chromatography with ammonium acetate and 1% acetonitrile. Because of the problem of contamination of the samples by the ammonium acetate, later isolation employed the Alltech C-8 semiprep column and HPLC Method C. In the latter case, UA–thymidine adduct I and UA–thymidine adduct II were collected at 8.4 (25 mL) and 12.6 min (38 mL), respectively. The adducts were freed from inorganic salts by lyophilization and a second pass

(9) Leighton, W. G.; Forbes, G. S. *J. Am. Chem. Soc.* **1930**, *52*, 3139–3152.

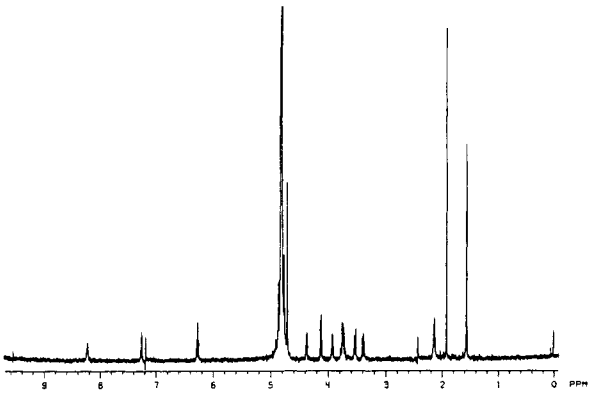

Figure 2. $^1H$ NMR spectrum of UA–thymidine adduct I.

through the semiprep column using pure water as eluent, after which both samples were found to be pure by HPLC analysis.

**(iii) Exact Mass Analysis.** Both UA–thymidine products were analyzed in a glycerol matrix by using high-resolution FAB mass spectrometry. The M + $H^+$ peaks for products I and II were found to be 381.1413 and 381.1398, respectively, *consistent with UA–thymidine cyclobutane adducts* (M + $H^+$ calculated to be 381.1410).

**(iv) Cleavage by 254-nm Photolysis.** Dilute solutions of adducts I and II in 0.02 M phosphate buffer (pH = 7) were irradiated for up to 60 s by using a low-pressure Hg lamp (254 nm). The photolysis solutions were analyzed by reverse-phase HPLC using an Alltech C-8 semiprep column (10 mm × 25 cm) and HPLC method D. Both adducts produced thymidine and, almost exclusively, (*E*)-UA upon initial photolysis. The amount of (*Z*)-UA increased with respect to (*E*)-UA upon further irradiation (the *Z* isomer is stable in the dark). *These results indicate that both adducts are cyclobutane structures derived from UA and thymidine.*[10] Furthermore, *the almost exclusive formation of (E)-UA upon initial photolysis suggests a trans relationship between the imidazole ring and the carboxylate functional group in both adducts.*[11] Further evidence for this relative stereochemistry in both adducts is presented below.

**(v) UV Spectra .** The UV spectra of the isolated adducts are similar and show only end absorption between 190 and 250 nm. *The disappearance of the ca. 270-nm bands of UA and thymidine confirms the disruption of conjugation in both initial chromophores, and the end absorption, characteristic of an isolated imidazole, is consistent with the formation of cyclobutane adducts from the acrylic acid double bond of UA and the 5,6 double bond of thymidine.*

**(vi) First-Order NMR Analysis.** Dilute samples of each adduct in 0.04 M phosphate buffer (pH = 6) were lyophilized and redissolved in 99.8% D $D_2O$. A second lyophilization was followed by the additon of 99.996% D $D_2O$ under an argon atmosphere. $^1H$ NMR spectra were acquired for both adducts by using the Nicolet NT-470 spectrometer with DSS as an internal reference. The $^{13}C$ NMR spectrum of UA–thymidine adduct I was obtained by using the Varian XL-200 spectrometer. The $^{13}C$ NMR spectrum of UA–thymidine adduct II was obtained by using the General Electric QE-300 spectrometer with DSS as the internal reference. The NMR spectra for both adducts are shown in Figures 2–5.

(10) Other UA cyclobutane adducts have been cleaved with 254-nm light; cf. ref 12.

(11) As predicted by orbital symmetry consideration, assuming the retro-cycloaddition is a concerted process.

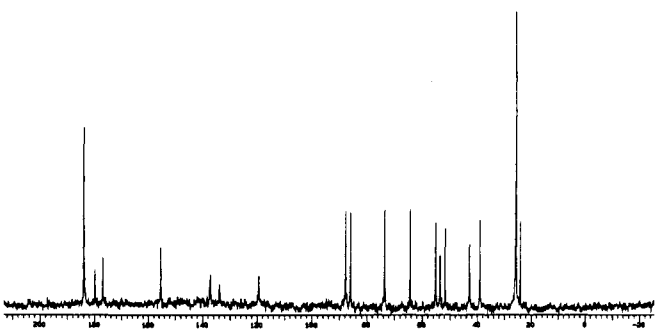

Figure 3. $^{13}C$ NMR spectrum of UA–thymidine adduct I.

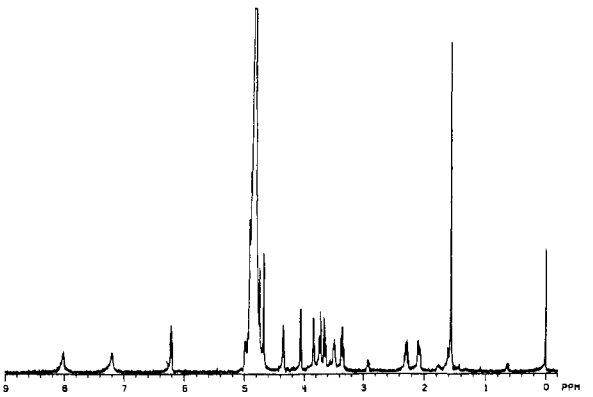

Figure 4. $^1H$ NMR spectrum of UA–thymidine adduct II.

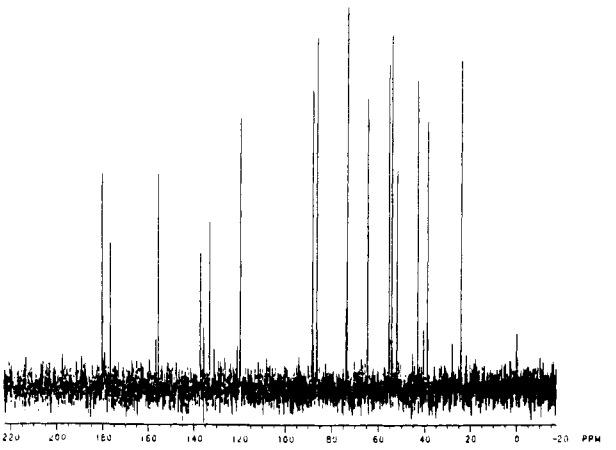

Figure 5. $^{13}C$ NMR spectrum of UA–thymidine adduct II.

*NMR data for both adducts are strikingly similar and are consistent with cyclobutane structures.* Missing in the spectra are the vinyl hydrogens of (*E*)-UA (δ 6.48 and 7.25) and the pyrimidine hydrogen of thymidine (δ 7.66). Concurrent with the loss of these downfield hydrogens is the appearance of three resonances with chemical shifts between δ 3.3 and 4.5 and with splitting patterns characteristic of a cyclobutane ring. Two hydrogens appear as two doublets with the other hydrogen represented as a doublet of doublets. Comparable changes occur in the $^{13}C$ spectra of both adducts. Thus, the resonances corresponding to the olefinic carbons of UA and thymidine are missing, and four new resonances appear between δ 40 and 60, consistent with UA–cyclobutane adducts.[12] The chemical shifts for the methyl hydrogens and the mehtyl carbons are virtually the same for both adducts and are shifted upfield relative to the methyl chemical shifts of

(12) Morrison, H. A.; Bernasconi, C.; Pandey, G. *Photochem. Photobiol.* **1983**, *38*, 23–27.

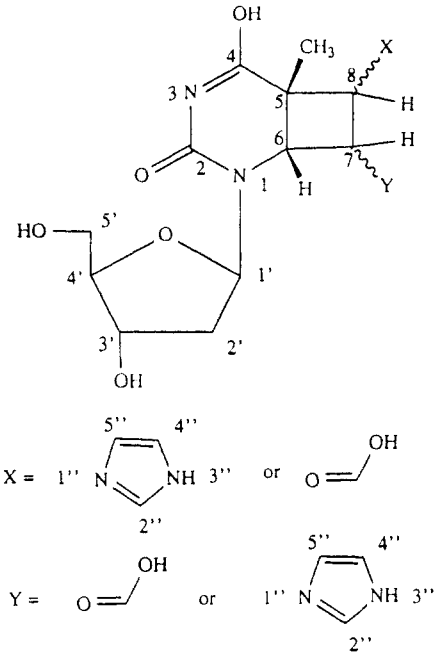


**Figure 6.** General structure and numbering scheme for the UA–thymidine adducts.

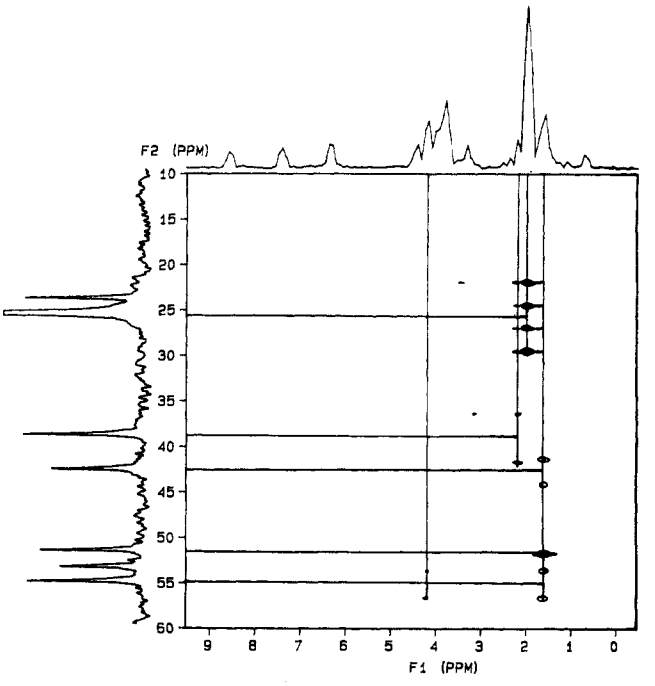


**Figure 7.** COLOC spectrum of UA–thymidine adduct I from 10 to 60 ppm.

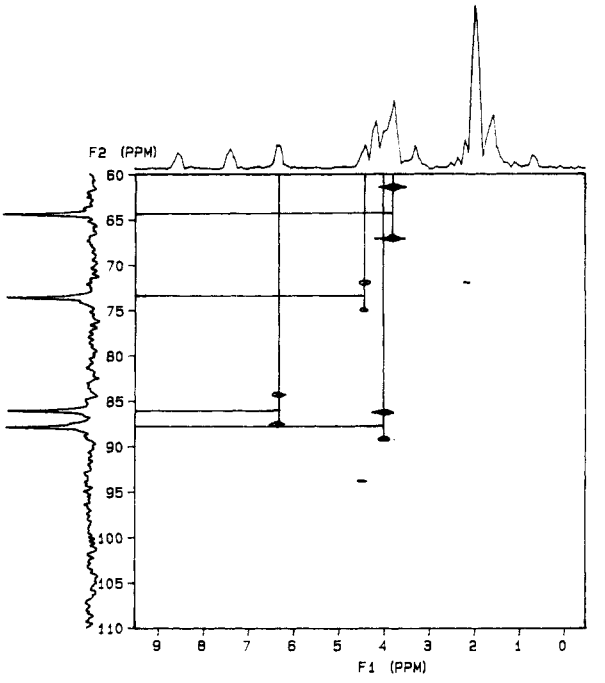


**Figure 8.** COLOC spectrum of UA–thymidine adduct I from 60 to 110 ppm.

thymidine. The upfield shift of the methyl group confirms the saturation of the pyrimidine ring and establishes the 5,6 double bond as part of the cycloaddition reaction.

The most obvious differences in the NMR data of the two UA–thymidine adducts occur in the proton chemical shifts of the deoxyribose hydrogens. For UA–thymidine adduct I, each set of diastereotopic hydrogens, H-2′ and H-5′, is a multiplet with chemical shifts at $\delta$ 2.13 and at 3.73, respectively. For UA–thymidine adduct II, each diastereotopic hydrogen has a unique chemical shift with the H-2′ hydrogens at $\delta$ 2.07 and 2.28, and the H-5′ hydrogens at $\delta$ 3.64 and 3.73. Both spectra differ from the spectrum of thymidine, which has unique chemical shifts for the H-5′ hydrogens but identical chemical shifts for the H-2′ hydrogens. The other deoxyribose chemical shifts in both the proton and carbon NMR spectra of the UA–thymidine adducts differ very little from the analogous shifts in thymidine.

**B. Detailed Characterization of the UA–Thymidine Adducts.** The results presented in the preceding section indicate that the two main photoproducts formed between (*E*)-UA and thymidine are both cyclobutane adducts. The general structure and numbering scheme used in the more detailed analysis below is shown in Figure 6. The results presented in this section allow for the unambiguous assignment of chemical shifts, regiochemistry, and relative stereochemistry.

**(i) Analysis of UA–Thymidine Adduct I Using Correlation Spectroscopy via Long-Range Couplings (COLOC).** The chemical shift data were acquired by using correlation spectroscopy on adduct I.[13] The sample was analyzed by heteronuclear shift correlation via small coupling constants, *without* broad-band decoupling during acquisition, and by using a constant delay (D3) of 35 ms.[14] The results are arranged as a set of three 2-D spectra in Figures 7–9, in which the scale for the $^{13}C$ NMR spectrum has been sectioned and correlated to a full proton spectrum. Because the decoupler was turned off during acquisition, the cross peaks provide information concerning the proton–carbon couplings for each carbon detected. The pulse sequence (COLOC) was optimized for long-range proton–carbon couplings, and two of the direct proton–carbon couplings are missing. Those direct couplings that are observed provide sufficient information to make complete chemical shift assignments, while the long-range couplings can be used to confirm the cyclobutane structure in the adduct.

Figure 7 represents the carbon NMR spectrum from 10 to 60 ppm correlated to a full proton spectrum and shows six proton–carbon couplings. The dominant interaction, a set of four cross peaks, is due to the direct proton–carbon

(13) The sample contained a small amount of acetic acid as an impurity.

(14) Kessler, H.; Griesinger, C.; Zarbock, J.; Loosli, H. R. *J. Magn. Reson.* **1984**, *57*, 331–336.

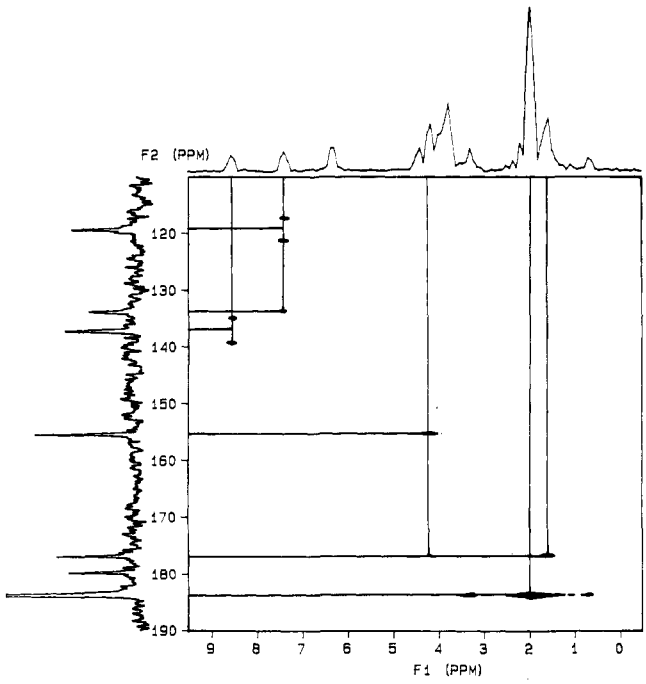


**Figure 9.** COLOC spectrum of UA–thymidine adduct I from 115 to 185 ppm.

coupling of acetic acid, a residual impurity from the chromatography eluent. There is a direct proton–carbon coupling for the hydrogens buried at δ 2.13 (the 2′ protons of the deoxyribose ring) and the C-2′ carbon at δ 39.08, giving rise to two peaks separated by twice the typical one-bond coupling constant. The center peak of this triplet is missing, as expected, due to the antiphase character of these cross peaks. There are also two cross peaks representing the direct proton–carbon coupling between the resonance at δ 4.11 (the more downfield of the two cyclobutane doublets and assignable to H-6) and the C-6 carbon resonance at δ 55.21. The three remaining sets of cross peaks are due to long-range proton–carbon couplings between the methyl hydrogens and the cyclobutane carbon resonances at δ 42.88 and 55.21 (two cross peaks each) and 51.80 (a single cross peak). The latter can be attributed to C-5 since this is the only cyclobutane carbon that does not bear a hydrogen. As regards the carbon at δ 42.88, the choice is between C-7 and C-8, with only C-8 lying within three bonds of the methyl hydrogens and therefore capable of giving the observed cross peaks. (The three-bond limitation arises because the area peak intensity decreases substantially as the long-range coupling constants become very small.) By elimination, the δ 53.63 resonance must be from C-7.

The region between 60 and 110 ppm in Figure 8 includes only direct proton–carbon connectivities of the deoxyribose group, the proton chemical shifts for which are well precedented. There is one set of two cross peaks with the center peak missing which must be due to the two H-5′ resonances around δ 3.73 and the C-5′ carbon resonance at δ 64.40. The other correlations all consist of two cross peaks and establish the resonances of C-3′ at δ 73.59 (H-3′ hydrogen at δ 4.36), C-1′ at δ 86.06 (H-1′ at δ 6.25), and C-4′ at δ 87.85 (H-4′ hydrogen at δ 3.92).

Figure 9 includes the region between 115 and 185 ppm and contains both direct and long-range proton carbon connectivities. Two direct couplings give rise to sets of two cross peaks involving the H-5″ and H-2″ imidazole resonances at δ 7.24 and 8.22, respectively, and establish C-5″ at δ 119.40 and C-2″ at δ 137.27. The other imidazole

**Table I. $^1$H NMR Chemical Shifts (δ)[a] and Coupling Constants of UA–Thymidine Adducts**

| assgnt | UA–thymidine I[b] | UA–thymidine II[c] |
|---|---|---|
| $CH_3$ | 1.55 s (3 H) | 1.55 s (3 H) |
| H-2′ | 2.13 m (2 H) | 2.07 m (1 H)<br>2.28 m (1 H) |
| H-7 | 3.38 dd (1 H, $J_{7,6}$ = 8.2, $J_{7,8}$ = 10.4 Hz) | 3.34 dd (1 H, $J_{7,6}$ = 8.7, $J_{7,8}$ = 10.3 Hz) |
| H-8 | 3.52 d (1 H, $J_{8,7}$ = 10.7 Hz) | 3.48 d (1 H, $J_{8,7}$ = 10.8 Hz) |
| H-5′ | 3.73 m (2 H) | 3.64 m (1 H)<br>3.73 m (1 H) |
| H-4′ | 3.92 m (1 H) | 3.83 m (1 H) |
| H-6 | 4.11 d (1 H, $J_{6,7}$ = 8.1 Hz) | 4.05 d (1 H, $J_{6,7}$ = 8.2 Hz) |
| H-3′ | 4.36 m (1 H) | 4.34 m (1 H) |
| H-1′ | 6.25 t (1 H) | 6.21 dd (1 H) |
| H-5″ | 7.24 s (1 H) | 7.20 s (1 H) |
| H-2″ | 8.22 s (1 H) | 8.01 s (1 H) |

[a] δ DSS = 0.00. [b] pH* = 6.4. [c] pH* = 6.6.

**Table II. $^{13}$C NMR Chemical Shifts of UA–Thymidine Adducts[a]**

| assgnt | UA–thymidine I | UA–thymidine II |
|---|---|---|
| $CH_3$ | 24.08 | 24.14 |
| C-2′ | 39.08 | 38.76 |
| C-8 | 42.88 | 42.96 |
| C-5 | 51.80 | 51.87 |
| C-7 | 53.63 | 54.08 |
| C-6 | 55.21 | 55.34 |
| C-5′ | 64.40 | 64.53 |
| C-3′ | 73.59 | 73.25 |
| C-1′ | 86.06 | 86.34 |
| C-4′ | 87.85 | 88.18 |
| C-5″ | 119.40 | 119.50 |
| C-4″ | 133.88 | 133.00 |
| C-2″ | 137.27 | 137.06 |
| C-2 | 155.44 | 155.38 |
| C-4 | 176.88 | 176.62 |
| $CO_2H$ | 179.85 | 180.25 |

[a] $^{13}$C NMR data were acquired at pH* = 6.4–6.6.

resonance at δ 133.88 must be C-4″; it gives rise to a single cross peak (and therefore has no directly bonded proton) as a result of long-range coupling to the H-5″ hydrogen at δ 7.24. The remaining correlations in Figure 9 are all long-range couplings and involve sp$^2$ hybridized carbons. The carbon resonance at δ 176.88 is coupled to both the H-6 hydrogen at δ 4.11 and the methyl hydrogens at δ 1.55 and is thus assignable to C-4 (the only sp$^2$ carbon within three bonds of both hydrogens regardless of whether the carboxylate group is attached to C-7 or C-8). The other two resonances at δ 155.44 (single cross peak to H-6) and 179.85 (no observed coupling) are assigned to C-2 and the carboxylate group, respectively. (The acetic acid carboxylate carbon resonance is found at δ 183.83.) A summary of the assigned proton chemical shifts for adducts I and II is presented in Table I, with the corresponding carbon shifts shown in Table II. It is interesting to note that the chemical shifts for the thymidine sp$^2$ carbons differ by ca. 20 ppm with the downfield shift observed for C-4 comparable to that seen for a carboxylic acid. This may be rationalized by proposing that both adducts are tautomerized, as shown in Figure 6.

**(ii) Regiochemistry of the UA–Thymidine Cyclobutane Adducts.** The regiochemistry for each adduct was determined by utilizing the pH dependence of the cyclobutyl proton chemical shifts. Both the imidazole ring and the carboxylate group attached to the cyclobutane ring

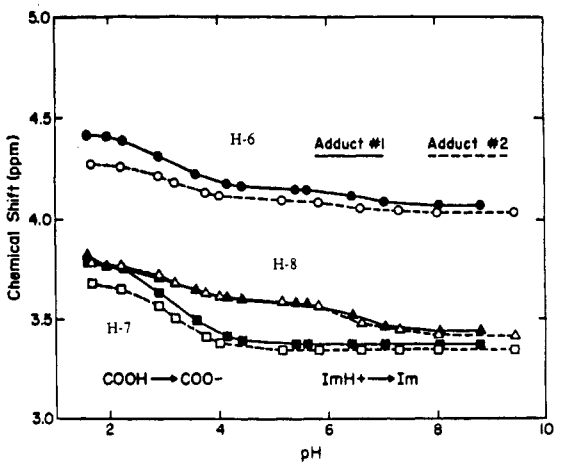


**Figure 10.** Chemical shift versus pH* for the UA–thymidine adducts.

**Table III. Effect of pH* on the Chemical Shifts of the Cyclobutane Hydrogens of the UA–Thymidine Adducts**

| H | pH* range | UA–thymidine I ($\Delta\delta$) | UA–thymidine II ($\Delta\delta$) |
|---|---|---|---|
| H-8 | 1.5–5.0 | 0.18 | 0.20 |
| | 5.0–9.0 | 0.16 | 0.17 |
| H-7 | 1.5–5.0 | 0.40 | 0.33 |
| | 5.0–9.0 | 0.02 | 0.00 |
| H-6 | 1.5–5.0 | 0.25 | 0.18 |
| | 5.0–9.0 | 0.08 | 0.06 |

have p$K$ values between 3 and 8. It is therefore reasonable to expect that the chemical shift of the hydrogen bonded to the carbon bearing the carboxyl group should show an upfield shift between pH 2 and 4 while the hydrogen bonded to the carbon bearing the imidazole ring should show an upfield shift between pH 5 and 7. The former effect is clearly seen in the NMR spectra of cyclobutanecarboxylic acid between pH* 1.0 and 5.0. Though all hydrogens are moved upfield, the effect on the chemical shift of the $\alpha$ hydrogen is ca. twice that seen for the $\beta$ or $\gamma$ hydrogens ($\delta$ −0.19 vs −0.08). Furthermore, there are relatively small changes in chemical shifts between pH* 5.0 and 13.5. Samples of each UA–thymidine adduct were dissolved in 99.996% D $D_2O$ with DSS as an internal standard, and the proton NMR spectra recorded at different pH* values by adding either DCl or NaOH in $D_2O$ directly into the NMR tube. The changes in chemical shifts for H-6, H-7, and H-8 are plotted as a function of pH* in Figure 10. The cumulative changes in chemical shifts from pH* 1.5 to 5.0 and 5.0 to 9.0 are summarized in Table III. These are the two pH* ranges that correspond to deprotonation of the carboxyl and imidazolium ion, respectively.

The data for the two adducts show similar trends in $\Delta\delta$ for each of the cyclobutane hydrogens. Though the chemical shifts for all three hydrogens are affected between pH* = 1.5 and pH* = 5.0, the greatest effect is at H-7 (shifted 0.40 and 0.33 ppm in adduct I and II, respectively). It is important to note that it is this hydrogen that shows little or no change in chemical shift between pH* = 5.0 and pH* = 9.0. H-6 responds similarly to H-7 but more modestly in the pH* 1.5–5.0 region, where deprotonation of the carboxyl group is occurring. Only H-8 responds significantly between pH* 5.0 and 9.0 (shifted 0.16 and 0.17 ppm for adducts I and II, respectively), the response between pH* 1.5 and 5.0 being comparable to H-6. We conclude that the carboxylate and imidazole groups are attached to C-7 and C-8, respectively, in both adducts (see Figure 11).

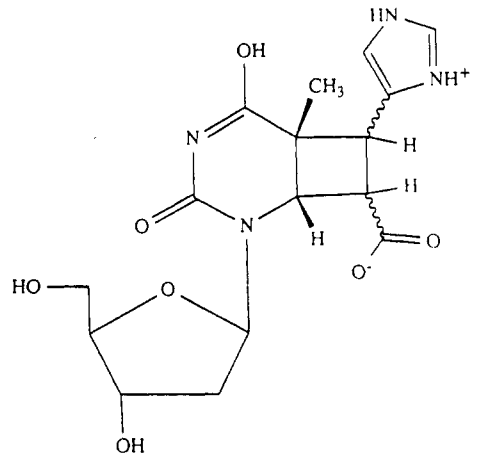

**Figure 11.** Regiochemistry of the UA–thymidine adducts.

**Table IV. Nuclear Overhauser Effects (NOE) for the UA–Thymidine Adducts**

| satd reson | obsd reson | % enhancement adduct I | % enhancement adduct II |
|---|---|---|---|
| $CH_3$ | H-7 | *a* | *a* |
| | H-8 | 4.5 | 3.8 |
| | H-6 | 2.8 | 1.9 |
| H-7 | $CH_3$ | *a* | *a* |
| | H-8 | *a* | *a* |
| | H-6 | 2.3 | *a* |
| | H-5″ | 10.4 | 6.6 |
| H-8 | $CH_3$ | 3.6 | 2.6 |
| | H-7 | *a* | 2.9 |
| | H-6 | *a* | 1.4 |
| | H-5″ | 3.5 | 1.0 |
| H-6 | $CH_3$ | 3.3 | 3.2 |
| | H-2′ | 3.2 | 4.4[b] |
| | H-7 | 4.2 | 7.7 |
| | H-8 | 7.0 | 5.1 |
| | H-1′ | *a* | 1.6 |
| H-1′ | H-2′ | 3.9 | 4.1[c] |
| | H-4′ | 2.9 | 3.2 |
| | H-7 | *a* | 4.3 |
| | H-6 | 1.6 | *a* |
| H-5″ | H-7 | 9.5 | 9.3 |
| | H-8 | 2.2 | 1.7 |
| | H-6 | *a* | *a* |
| H-2″ | H-7 | *a* | 3.8 |
| | H-5″ | 1.9 | *a* |

[a] No enhancement was observed. [b] Enhancement of H-2′ at $\delta$ 2.28. [c] Enhancement of H-2′ at $\delta$ 2.07.

**(iii) Stereochemistry of the Adducts. Nuclear Overhauser Effect (NOE) Experiments.** NOEs were acquired by using the difference method, whereby one resonance is saturated and the effects on the intensities of other resonances are compared to equilibrium values.[15] Dilute samples of each adduct in 0.04 M phosphate buffer (pH = 6) were lyophilized and redissolved in 99.8% $D_2O$. A second lyophilization was followed by the addition of 99.996% D2O under an argon atmosphere. A series of data was collected at 470 MHz for each adduct by saturating either the methyl group, H-7, H-8, H-6, H-1′, H-5″, or H-2″ and determining the effect on other hydrogens in the molecule. Our results are presented in Table IV. NOEs between the methyl group and the $H_6$ and $H_8$ resonances are noteworthy in that they suggest that these two hydrogens and the methyl group are on the same face of the cyclobutane ring in both adducts.

(15) Derome, A. E. *Modern NMR Techniques for Chemistry Research*; Pergamon Press: New York, 1987; pp 97–127.

Table V. $T_1^{SE}$ Values for the UA-Thymidine Adducts

| H | $T_1^{SE}$, s adduct I | $T_1^{SE}$, s adduct II | H | $T_1^{SE}$, s adduct I | $T_1^{SE}$, s adduct II |
|---|---|---|---|---|---|
| $CH_3$ | 0.53 | 0.53 | H-1′ | 1.9 | 1.4 |
| H-7 | 1.9 | 2.0 | H-5″ | 2.3 | 2.4 |
| H-8 | 1.4 | 1.4 | H-2″ | 2.4 | 3.0 |
| H-6 | 0.94 | 0.84 | | | |

To examine this issue more carefully, we also measured several single-resonance-selective inversion recovery spin–lattice relaxation times, $T_1^{SE}$,[15] these are presented in Table V. Note that the $T_1^{SE}$ value for the $H_6$ resonance is a bit smaller than for $H_8$. This compensates for the smaller NOE observed at $H_6$. In fact, this comparison can be put on a more quantitative basis[16] since, for simple motional models, eq 1 holds. With this relationship, the data in

$$r^6 \propto T_1^{SE}/\mathrm{NOE} \quad (1)$$

Tables IV and V can be used to quantitate the strength of various dipole–dipole interactions and give ratios of interproton distances. The $T_1^{SE}$ values and the NOEs observed at the $H_6$ and $H_8$ resonances upon saturation of the methyl resonance give a ratio of 1.02 for the methyl–$H_6$ and methyl–$H_8$ distances. This confirms that $H_6$ and $H_8$ are equidistant from the methyl group and the conclusion indicated above that they are on the same face of the cyclobutane ring. Furthermore, using the $T_1^{SE}$ and NOE data to compare the strength of dipole–dipole interactions throughout the molecule shows that the interactions between both $H_6$ and $H_8$ and the methyl group are the strongest we observe in the molecule. This is the case regardless of whether NOEs are observed at the methyl resonance when $H_6$ or $H_8$ is saturated or if the $H_6$ or $H_8$ resonance is observed and the methyl resonance saturated. This further supports placing $H_6$ and $H_8$ on the face of the cyclobutane ring as the methyl group.

On the other hand, we do not see NOEs between $H_7$ and the methyl group, a fact consistent with chemical reasoning that the protons that become $H_7$ and $H_8$ retain, upon cycloaddition, the trans relationship originating in (*E*)-UA. This orientation of $H_7$ is further supported by the very strong NOEs between $H_7$ and $H_{5''}$.

In summary, we have found a striking similarity of both the carbon and proton chemical shifts in the spectra of the two adducts, identical regiochemistry, and comparable NOE and $T_1$ data (and thus relative stereochemistry). *We are therefore led to conclude that the two cyclobutane adducts are diastereomers.*

**(iv) Acid Hydrolysis of the UA–Thymidine Adducts.** If adducts I and II are diastereomerically related, cleavage of the N-glycosidic linkage in the two adducts should result in a pair of enantiomers with identical HPLC retention times.[17] Both UA–thymidine adducts were, therefore, hydrolyzed by dissolving 0.5 mg in 0.3 mL of 2.7 N HCl and heated at 70 °C for 30 min. The hydrolysis solutions were analyzed by reverse-phase HPLC using method E and found to exhibit similar HPLC traces with evidence for a single (UA–thymine) adduct peak. That this peak was indeed due to a UA–thymine adduct was confirmed by collecting the peak from both hydrolyses and photolyzing in each case with $\lambda$ = 254 nm light. Reinjection of the solutions indicated that cleavage to (*Z*)-UA and thymine had occurred.[18] The product peaks isolated from the two hydrolysis solutions were analyzed by using several additional HPLC conditions but in all events demonstrated identical retention times, and their coinjection resulted in a single, sharp peak with no visible shoulders or broadening.[19] These results provide strong support for the proposal that the two UA–thymidine adducts are indeed diastereomers (see Figure 12).

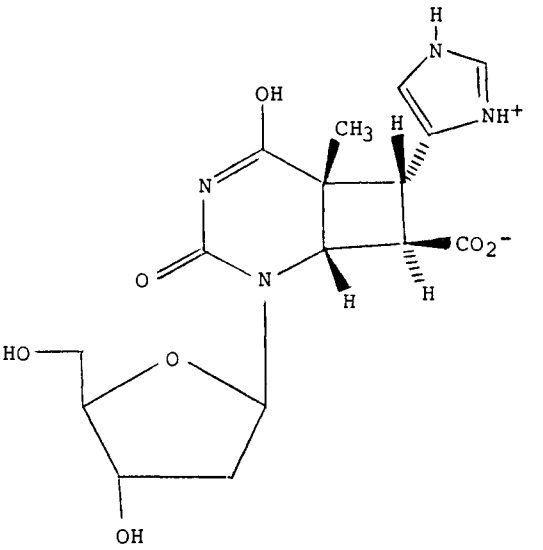


**Figure 12.** One (i.e., 5*R*,6*S*) of the two diastereomeric UA–thymidine adducts. The second adduct has the 5*S*,6*R* configuration.

Table VI. Estimated Distances (angstroms) for Hydrogens in UA–Thymidine Adducts by Using MacroModel

| hydrogen A | hydrogen B | A–B dist,[a] Å ImH$^+$/$CO_2^-$ isomer 1 | ImH$^+$/$CO_2^-$ isomer 2 | ImH$^+$/$CO_2$H isomer 1 | ImH$^+$/$CO_2$H isomer 2 |
|---|---|---|---|---|---|
| CH3 | H-8 | 2.39 | 2.37 | 2.36 | 2.37 |
| CH3 | H-7 | 4.44 | 4.43 | 4.36 | 4.30 |
| CH3 | H-6 | 2.38 | 2.38 | 2.34 | 2.37 |
| H-8 | H-7 | 3.06 | 3.06 | 3.02 | 3.02 |
| H-8 | H-6 | 2.63 | 2.74 | 3.05 | 3.18 |
| H-7 | H-6 | 3.07 | 3.05 | 3.05 | 3.02 |
| H-6 | H-1′ | 3.52 | 3.74 | 3.45 | 3.76 |
| H-6 | H-2′ | 3.51 | 2.35 | 3.74 | 2.45 |
| H-7 | H-1′ | 4.46 | 3.87 | 4.25 | 3.45 |
| H-7 | H-2′ | 2.86 | 4.75 | 2.36 | 4.59 |
| H-6 | H-5″ | 5.40 | 5.32 | 5.14 | 5.14 |
| H-7 | H-5″ | 4.39 | 4.39 | 2.60 | 2.52 |
| H-8 | H-5″ | 3.39 | 3.40 | 3.32 | 3.33 |

[a] The values given for methyl and methylene hydrogens are the shortest distances calculated.

**(v) Modeling of the UA–Thymidine Adducts.** The two possible diastereomers (isomer 1, 5*R*,6*S*; isomer 2, 5*S*,6*R*) were optimized as the zwitterion by using a series of rotamers about the N-glycosidic bonds. The conformatioonal energies were minimized on a MicroVAX II (VMS Version 4.6) using MacroModel Version 2.0[20] and the MM2 (85) Force Field.[21] The lowest energy structures for the two stereoisomers were evaluated for bond distances by using MIND, an interactive molecular display program.[22] Since no solvent was included in the calculation, a second calculation was done with a "protonated"

(16) Jones, C. R.; Sikakana, C. T.; Hehir, S. P.; Kan, M. C.; Gibbons, W. A. *Biophys. J.* **1978**, *24*, 815–832.
(17) See, for example: Cadet, J.; Voituriez, L.; Hruska, F. E.; Kan, L.; De Leeuw, F. A. A. M.; Altona, C. *Can. J. Chem.* **1985**, *63*, 2861–2868.
(18) (*E*)-UA has the same retention time as the UA–thymine adduct under these conditions so that only (*Z*)-UA would be detectable.
(19) There was, unfortunately, insufficient material for optical rotation measurements.
(20) Still, W. C. *Macromodel. Version 1.5*; Columbia University: New York, 1987.
(21) Allinger, N. L. *J. Am. Chem. Soc.* **1977**, *99*, 8127–8134.
(22) This program was developed by Julian Tirado-Rives and James F. Blake from Purdue University.

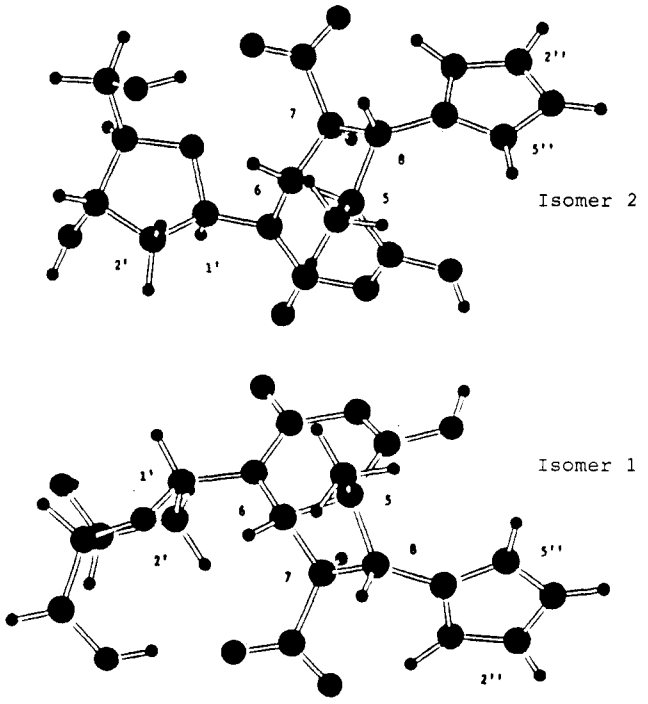


**Figure 13.** Optimized structures for stereoisomers 1 and 2 with $ImH^+/CO_2^-$.

carboxylate to simulate the effect of hydrogen bonding of the zwitterion in water. Interatomic distances were determined for various pairs of hydrogens (Table VI), and the optimized structures for each stereoisomer have been plotted in Figures 13 ($ImH^+/CO_2^-$) and 14 ($ImH^+/CO_2H$).

It is interesting to note that optimization with the carboxylate group protonated leads to a pair of structures (Figure 14) in which the distances between H-5″ and the H-7 hydrogens are calculated to be ca. 2.5 Å, consistent with the large NOE effects reported in Table IV. By contrast, when the carboxylate group is deprotonated (Figure 13), these distances (ca. 4.4 Å) are relatively long and inconsistent with such large NOE effects.

**C. Quantum Efficiency of Reaction.** A 3-mL solution of (*E*)-[*ring*-2-$^{14}$C]urocanic acid (2 mM; SA = $2.7 \times 10^{-2}$ mCi/mmol) and thymidine (4 mM) in 0.1 M phosphate buffer (pH = 7) was irradiated with argon bubbling for 60.0 min by using the XeCl excimer laser ($\lambda$ = 308 nm). The light intensity of the laser was determined to be $4.6 \times 10^{17}$ $h\nu$/s, and showed little diminution during the course of the experiment. The reaction was analyzed by HPLC using the Alltech C-8 semiprep column and HPLC method C ($R_t$ (min) = adduct I, 8.0; adduct II, 12.0; (*E*)-UA, 6.3; (*Z*)-UA, 13.3; thymidine, 19.7. Under these photolysis conditions, the UA isomers and thymidine absorb 92% and 8% of the light, respectively. After photolysis, adduct I and adduct II comprised 1.0% and 1.4% of the total radioactivity, respectively, giving $\Phi_I = 2.1 \times 10^{-5}$ and $\Phi_{II} = 2.5 \times 10^{-5}$.[23] The quantum efficiency for UA disappearance ($\Phi_{dis}$) is $4.80 \times 10^{-4}$. The quantum efficiencies for adduct formation will, of course, be a function of reactant concentrations.

(23) Which, if not both, of the possible excited species is the excited reactant remains undefined. Evidence has been presented elsewhere[12] that supports the reaction, at least in part, from a thymine excited singlet state.

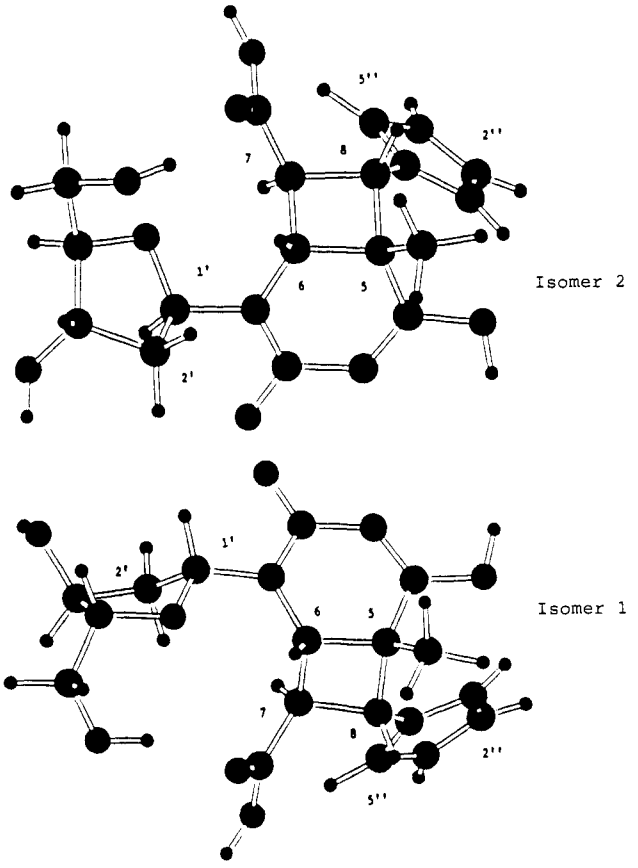


**Figure 14.** Optimized structures for stereoisomers 1 and 2 with $ImH^+/CO_2H$.

## Summary

Two diastereomeric cyclobutane photoadducts of (*E*)-urocanic acid and thymidine have been isolated and fully characterized. The formation of these products lends further support to the proposal[6] that the cycloaddition of UA with the pyrimidine bases is a major source of the UA-photoinduced lesions in DNA. Further studies on the mechanistic and photobiological implications of this photochemistry are in progress.

**Acknowledgment.** We thank the National Institutes of Health (Grant 5R01 CA 18267) for support of this research and the Purdue University Biomagnetic Resonance Laboratory (NIH Grant RR01077) for assistance in obtaining the high-field NMR spectra. We also thank Dr. Karl Wood and Gerry Olack for their assistance in obtaining the FAB spectra and portions of the NMR data, respectively, Professor William Jorgensen for the use of his Sun 4 computer for the modeling studies, and Professor Ed Grant for the use of the excimer laser.

**Registry No.** I, 123506-62-7; II, 123506-63-8; (*E*)-UA, 3465-72-3; thymidine, 50-89-5.